This is the accepted version of an article published in IEEE Transactions on Plasma Science
DOI: 10.1109/TPS.2018.2880841

Ultrahigh-Pressure Nitrogen Arcs Burning inside Cylindrical Tubes

Fahim Abid, Kaveh Niayesh, *Senior Member, IEEE*, Nina Støa-Aanensen

***Abstract*— When the pressure and temperature of a fluid exceed a critical point, the fluid enters into the supercritical region. In this region, the physical properties are believed to be in favor of a good current interruption medium. This study focuses on the arc voltage characteristics of nitrogen arcs burning inside cylindrical tubes at different filling pressures: 1 bar, 20 bar, 40 bar, and 80 bar, thus covering the supercritical region. Two different tube materials have been used in the experiments; alumina and PTFE. Arc voltages are measured for arcs burning inside tubes of 2, 4, 8, and 15 mm inner diameters. In addition, free-burning arcs have been investigated at the same filling pressures. The arc current was 150 A at 350 Hz throughout the study. The arc voltage is found to increase with decreasing inner diameter of the tube at atmospheric pressure. At higher filling pressures (i.e., 20 bar, 40 bar, 80 bar), however, such a simple relationship is not observed. The arc temperature and radius have been calculated based on the 'simple theory of free-burning arcs' and the 'two-zone ablation arc model'. The calculated arc radius decreases with increasing gas pressure. Furthermore, due to increased absorption of radiation at high filling pressures, ablation is found less significant for ultrahigh-pressure nitrogen arcs compared to atmospheric pressure arcs. This is in line with the observations from optical micrographs of the inner surfaces of the tubes exposed to arcs at different filling pressures.**

***Index Terms*— Arc voltage, supercritical nitrogen, switchgear, ultra-high pressure arc, two-zone arc model.**

I. Introduction

An increase of wind farms and mining operations located far off the coast will increase the need for offshore substations in the future. Such substations can be put on the seabed instead of building expensive floaters and platforms [1]. Placing the equipment on the seabed in many cases implies that it must be protected from water and the high ambient pressure at the seabed. Conventional switching equipment such as circuit breakers (vacuum breakers or breakers filled with gases at a few bars) require expensive solutions for encapsulation and feedthroughs to protect them from water and high ambient pressure. A novel concept based on filling the interrupting chamber with a fluid at the same high pressure as the surroundings could substantially reduce the cost of the encapsulations and feedthroughs.

Nitrogen (N_2) is a good insulating gas. When the pressure and temperature of N_2 exceed the critical pressure (33.5 bar) and temperature (126 K), it enters into the supercritical (SC) region [2]. Properties such as the density, viscosity, diffusivity, thermal conductivity, and heat capacity of SC N_2 are believed to be in favor of a good interruption medium [3]. However, electrical discharges inside SC N_2 are not a well-explored field because of the high pressure needed for the transition into the SC region. A few works have reported on electrical discharges inside supercritical fluids in general [4-8]. However, in contrast to the high energy (normally up to hundreds of kilojoules) deposited in switching arcs of medium voltage switchgears, previous studies cover short distance electrical discharges in SC fluids for energy dissipation in the range of millijoules.

The voltage drop across free-burning nitrogen arcs has been found to increase with increasing filling pressure without any abrupt change during the transition from gas to supercritical state [9]. In gas-filled circuit breakers, the arcs are usually not free-burning, but constricted by an insulating nozzle or tube. In contrast to free-burning arcs, a cylindrical tube constricts the diameter of the arc core based on the tube material and the inner diameter of the tube. A part of the radiation from the arc core transparently leaves the tube, while some part is absorbed at the boundary of the arc. The rest of the radiation reaches the inner surface of the tube, causing ablation. As the cylinder ablates, a high-pressure stagnation region is formed at the center of the tube, which expels the plasma out from both ends of the tube. Several works have been reported for such tube-constricted arcs at atmospheric pressure [10-14]. However, little or no work have been reported for arcs burning inside a tube at a very high filling pressure.

This paper focuses on the arc voltage characteristics of arcs burning inside cylindrical tubes at different filling pressures of N_2. The voltage drop for arcs burning in tubes with varied inner diameters are measured alongside those of free-burning arcs. The arcs burning inside tube at higher filling pressures are then compared with arcs burning in air at atmospheric pressure. To analyze ablation effects further, two different tube materials have been studied: ablating Polytetrafluoroethylene (PTFE), and a less-ablating ceramic material (alumina). To qualitatively evaluate the ablation caused by an arc at high filling pressures as well as at atmospheric pressure, the inner surface of the tubes are inspected using an optical microscope. Some of these works have been presented in a conference report [15].

The experimental setup and procedure are explained in chapter II, followed by the experimental results in chapter III. Using well-known semi-analytical arc models, the temperatures

F. Abid and K. Niayesh are with the Department of Electrical Power Engineering, Norwegian University of Science and Technology, 7491 Trondheim, Norway (e-mail: fahim.abid@ntnu.no).

N. S. Støa-Aanensen is with SINTEF Energy Research, 7465 Trondheim, Norway.

This is the accepted version of an article published in IEEE Transactions on Plasma Science
DOI: 10.1109/TPS.2018.2880841

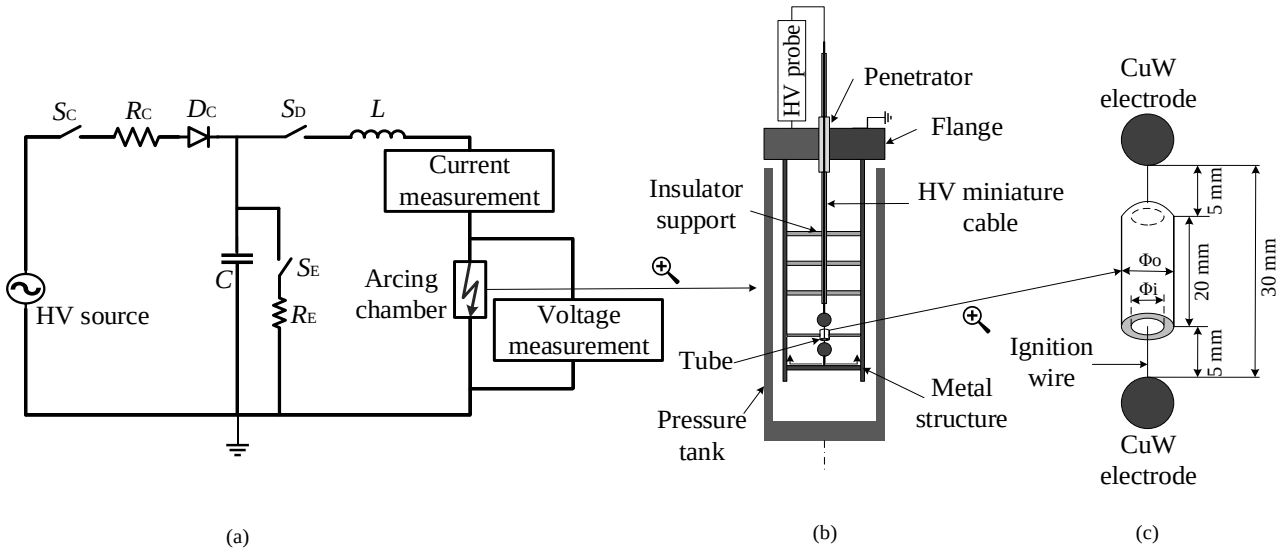

Fig. 1: The experimental setup. (a) The test circuit showing the charging and discharging part of the circuit. (b) Schematics of the high pressure arcing chamber and the inside connections. (c) The configuration of the tube with respect to electrodes inside the arcing chamber.

and radii of the arcs are calculated and discussed in chapter IV. Finally, based on the experimental results and discussions, the conclusions are drawn in chapter V.

II. Experimental Setup And Procedure

The experimental setup is shown schematically in Fig. 1. The test circuit consists of the charging and discharging sections of a 4.8 µF high voltage (HV) capacitor, *C*, shown in Fig. 1(a). The capacitor is charged to a predefined charging voltage of 15 kV through the diode resistor unit R_C-D_C. Once the capacitor is charged, the switch S_C is opened to disconnect the charged capacitor from the grid. Due to the decay of the charged voltage of the capacitor through internal stray resistance, a ±5% error in the charging voltage is present in the system. When the knife switch, S_D, is closed, the capacitor is discharged through the inductor, *L*, and further through an ignition wire in the arcing chamber. The ignition wire melts due to adiabatic heating within 0.1 ms, and the current continues to flow through an arc.

A pressure tank of 15.7-liters rated for 500 bar is used as arcing chamber, this is shown schematically in Fig. 1(b). Prior to each test, the pressure vessel is flushed with industrial grade nitrogen. It is ensured that 99% pure nitrogen is used for all the experiments conducted, except for atmospheric pressure cases, where ambient air is used. A 24 kV miniature HV cable is fed through the pressure tank (the techniques are described in [16]). The miniature cable is held in position by several insulating supports. In a previous study on free-burning arcs, it was reported that the copper vapor did not have a significant effect on the arc characteristics if the thickness of the ignition wire was kept less than 100 µm [9]. Hence, a copper wire with a diameter of 25 µm is used to initiate the arc. The ignition wire is passed through the tube and attached between two identical copper-tungsten (Cu-W) spherical electrodes of 10 mm diameter.

The insulating cylindrical tubes with a length of 20 mm and different inner diameters are held in position by an insulating support at a 5 mm distance from the electrodes, as shown in Fig. 1(c). The return path of the current is through the supporting metal structure and the flange of the pressure tank. An HV probe is used to measure the voltage across the electrodes and a shunt resistor is used to measure the current flowing through the arc.

TABLE I
Test Cases and Conditions.

Tube material	Current [A]	Tube diameter [mm]	Frequency [Hz]	Filling pressure [bar]
Alumina	150	2, 4, 8, 15	350	1, 20, 40, 80
PTFE	150	2, 4, 8, 15	350	1, 20, 40, 80
Free-burning	150	No tube	350	1, 20, 40, 80

Two different tube materials are investigated: PTFE and alumina. The inner diameter, Φ_i, is varied from 2 to 4, 8, and 15 mm. Corresponding experiments with free-burning arcs (without tube) are also carried out. The outer diameter of the tube, Φ_o, is either 15 mm (for the Φ_i= 2, 4, and 8 mm tubes) or 20 mm (for Φ_i= 15 mm tube). After each experiment, the tubes are carefully examined to ensure that no arc traces are found on their outer surfaces. The tubes are tested at four different filling pressures: 1 bar (atmospheric air), 20 bar, 40 bar, and 80 bar. Each test case is repeated three times. All the test cases are summarized in Table I.

The inner surfaces of the tubes are investigated by optical microscopy. After the arcing tests, three types of samples for both PTFE and alumina are studied using microscopy: without any arc (reference), after arcing at 1 bar, and after arcing at 80 bar N_2 for 4 mm inner diameter of the tube. To prepare the samples, the tubes are cut along the axis and cleaned with a soft brush to remove the arcing by-products. The microscopy samples are taken from the middle part of the inner surface of the tube.

This is the accepted version of an article published in IEEE Transactions on Plasma Science
DOI: 10.1109/TPS.2018.2880841

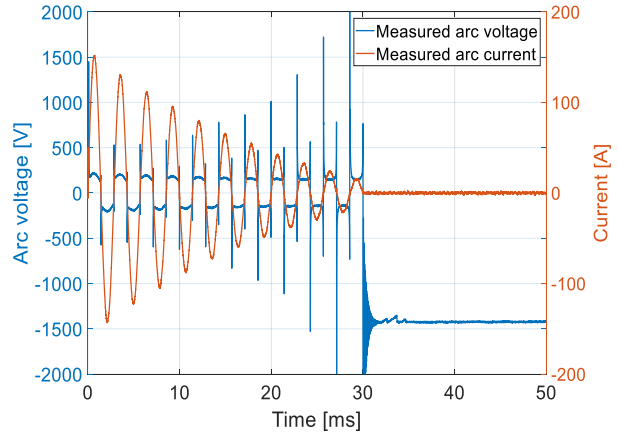

(a)

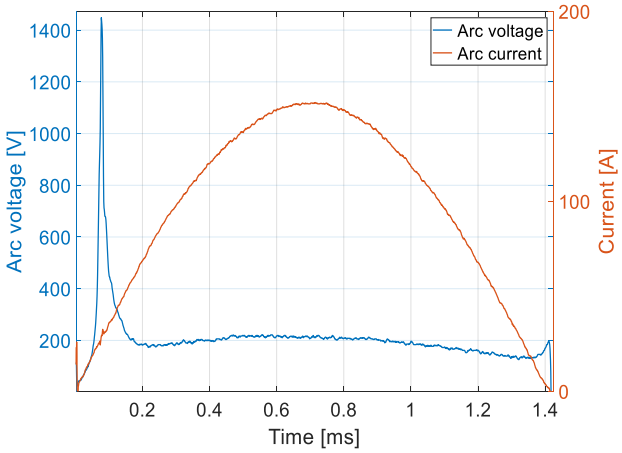

(b)

Fig. 2. Measured arc current and arc voltage waveform for arc burning inside 2 mm PTFE tube at atmospheric pressure. (a) The current is damped out due to the arc resistance. (b) First half cycle of the measured arc current and arc voltage.

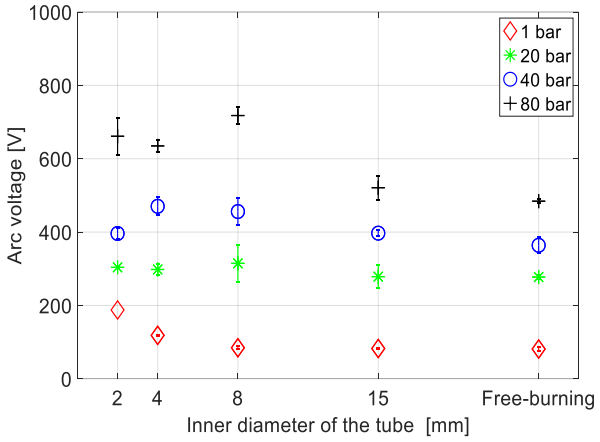

(a)

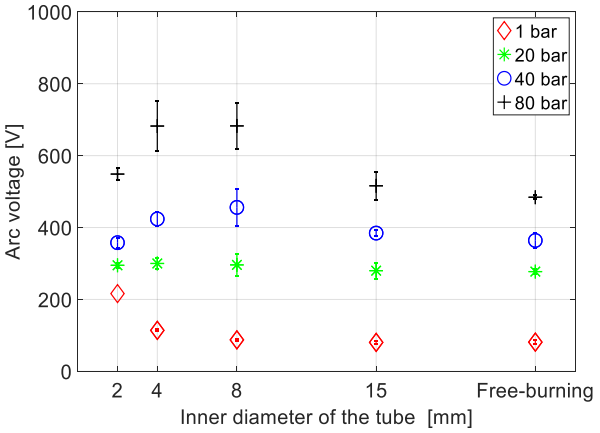

(b)

Fig. 3. Arc voltages at the current peak of 150 A at 350 Hz as a function of inner diameters of the tubes at different filling pressures. (a) Alumina. (b) PTFE.

III. Experimental Results

A typical arcing test with measurements of the arc voltage and the current for an arc burning inside a 2 mm PTFE tube at atmospheric pressure is shown in Fig. 2 (a). Due to the arc resistance, the current damps out with time. It has been reported that the arc resistance changes with gas pressure [9]. Therefore, only the first half cycle of the current is considered for further analysis. The current starts at t = 0, while the arc initiates at around t = 0.1 ms, when the ignition wire has melted (first voltage peak), see Fig. 2 (b). Once the arc is initiated, a stable arc voltage is measured from approximately 0.2 ms until it collapses before current zero. This paper investigates the arc voltage characteristics at the peak current of the first half cycle.

A. Arc Voltage Dependency on Inner Diameter of the Tube at Different Filling Pressures

The arc voltage as a function of the inner diameter of the tube for different filling pressures is plotted in Fig. 3, together with the free-burning arc tests. The average arc voltage of the three tests conducted per test case is plotted with an error bar. Here, the error bar is the maximum deviation from the average arc voltage per test case. Fig. 3(a) shows the arc voltages corresponding to alumina tubes, while the arc voltages inside the PTFE tubes are plotted in Fig. 3(b). At atmospheric pressure, the average free-burning arc voltage is found to be approximately 80 V. As the inner diameter decreases, a gradual increase of the arc voltage is observed for both alumina and PTFE tubes at 1 bar. The average arc voltage increases to 187 V for arcs burning inside a 2 mm wide alumina tube, and to 215 V for arcs burning inside a 2 mm wide PTFE tube at atmospheric pressure.

As the nitrogen filling pressure is increased, the arc voltage increases too. This is expected based on previous investigations [9]. The arc voltages measured for arcs burning inside 15 mm wide tubes are similar to those of corresponding free-burning arcs. The variation in arc voltage for a given case seems to increase somewhat with increasing pressure and decreasing diameter, although the data is limited. The arc voltage dependency on the tube material is not strong at 20, 40, and 80 bar nitrogen filling pressures.

The gradual increase in arc voltage with decreasing tube

This is the accepted version of an article published in IEEE Transactions on Plasma Science
DOI: 10.1109/TPS.2018.2880841

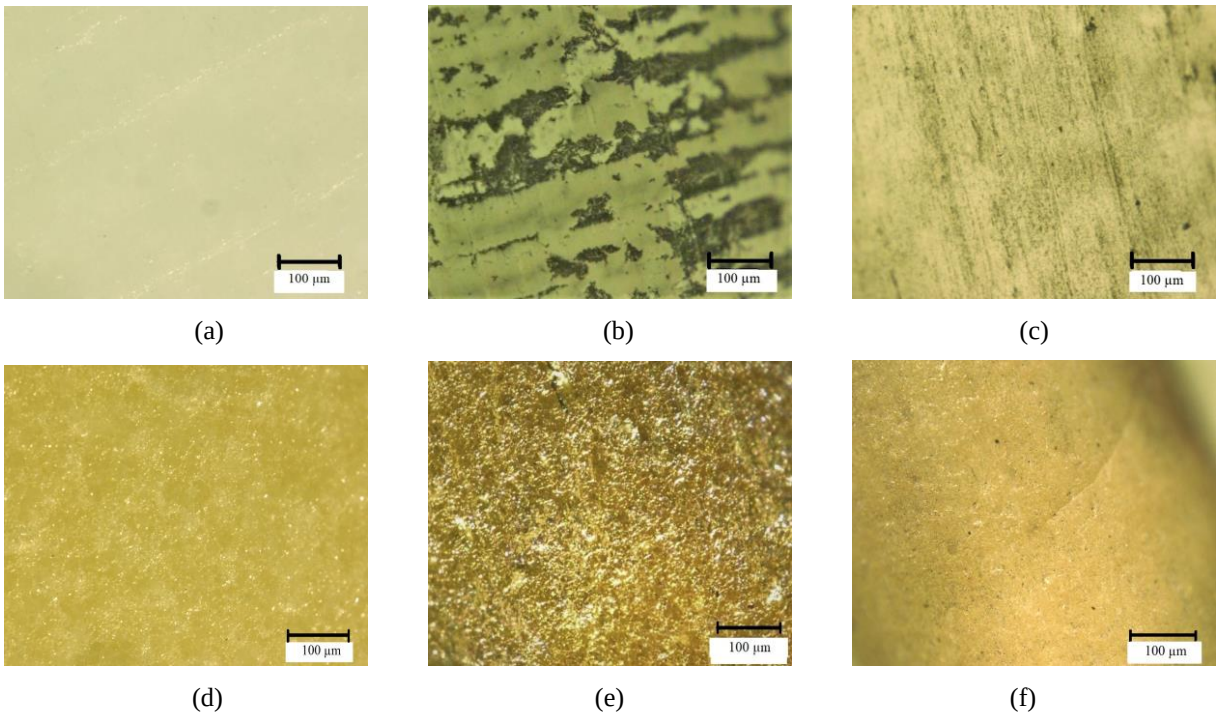

Fig. 4. Optical micrographs of the inner surface of 4 mm diameter tubes. (a) PTFE new (no arc). (b) PTFE, after arc at atmospheric pressure. (c) PTFE, after arc at 80 bar filling pressure. (d) Alumina new (no arc). (e) Alumina, after arc at atmospheric pressure. (f) Alumina, after arc at 80 bar filling pressure.

inner diameter that was observed for arcs at 1 bar pressure is not evident for higher pressures. At a nitrogen filling pressure of 20 bar, the arc voltage (approximately 300 V) seems to be more or less independent of both tube inner diameter and tube material. At 40, and 80 bar nitrogen, the maximum arc voltage is observed not for the smallest inner diameter of the tubes, but rather for 4 or 8 mm tube inner diameters.

B. *Optical Microscopy of the Inner Surface of the Tube*

Fig. 4 shows the optical micrographs of the investigated inner surfaces of tubes with 4 mm inner diameter before and after arcing. At atmospheric pressure, carbonization and scar marks are visible in the PTFE tube, (Fig. 4(b)). The presence of carbonization marks after arcing at atmospheric pressure could be due to the presence of O_2 and CO_2 in air. The ablation traces are significantly less visible in the PTFE tubes after arcing in 80 bar nitrogen, (Fig. 4(c)). When the arc burns inside alumina tubes at atmospheric pressure (Fig. 4(e)), the surface is changed compared to new alumina (Fig. 4(d)). On the other hand, when the filling pressure is increased to 80 bar, almost no arc traces are observed in the alumina tubes, as shown in Fig. 4(f). Both of the materials show reduced ablation traces at 80 bar nitrogen in contrast to atmospheric air.

IV. Model And Discussions

A. *Free-burning Arc*

The free-burning arc properties can be calculated based on Lowke's analytical model of free-burning arcs to estimate the effect of constriction due to the filling pressure [17]. The model is validated by comparing the calculated and the measured arc voltages. The peak arc current in this paper is 150 A, which is considered as a high-current arc. According to Lowke's model, the temperature at the arc center can be determined by the energy balance equation

$$\frac{I^2}{\sigma A^2} = \frac{4\pi k T}{A} + U, \tag{1}$$

where I is the arc current, σ is the electrical conductivity, A is the arc cross-sectional area, T is the temperature of the arc, k is the thermal conductivity, and U is the net radiation emission. The arc core is assumed to be a blackbody radiator and the net radiation emission can be expressed as

$$U = \frac{2\beta T^4}{r}\epsilon\,, \tag{2}$$

where β is the Stefan-Boltzmann constant, r is the arc radius, and ϵ is a parameter which characterizes the radiation mechanism inside the arc [12]. The parameter ϵ depends on the pressure and the arc radius and can be written as

$$\epsilon = 1 - \exp[-\gamma(pr)^{0.6}]\,, \tag{3}$$

where p is the pressure. The γ is a constant and has been considered equal to a value 0.025 by Niemeyer for a range of plastic materials [18]. However, for free-burning arcs in air, the constant γ is lower than 0.025. In this paper it is assumed to be 0.007 at atmospheric pressure and 0.023 at 80 bar based on the data for arcs burning in air [18].

The equations that define the arc radius and the electric field in the free-burning arc are taken directly from the expressions for high current arcs deduced by Lowke [17]:

This is the accepted version of an article published in IEEE Transactions on Plasma Science
DOI: 10.1109/TPS.2018.2880841

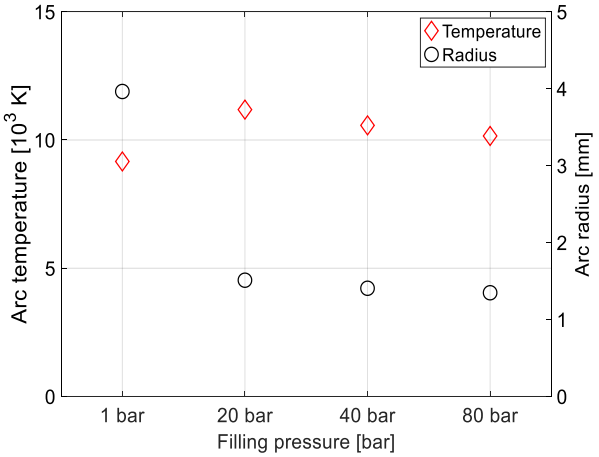

(a)

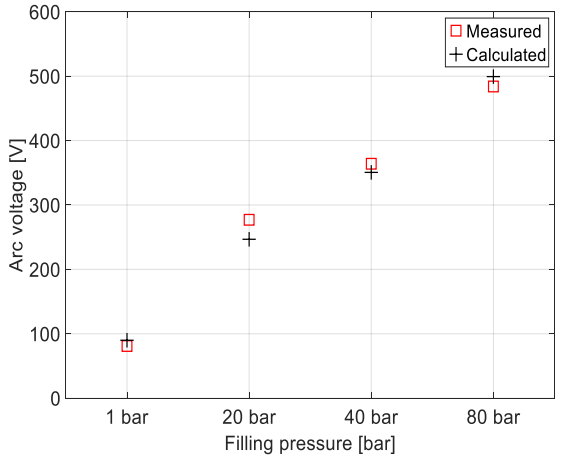

(b)

Fig. 5. Calculated parameters of free-burning arcs as a function of filling pressure for arc current of 150 A (a) Calculated arc temperature and radius. (b) Measured and calculated arc voltage.

$$r = 1.11\left(\frac{z}{h\sigma}\right)^{\frac{1}{4}}\frac{I^{\frac{3}{8}}}{(\mu J_o \rho)^{\frac{1}{8}}}, \tag{4}$$

and

$$E = 0.26\left(\frac{h}{z\sigma}\right)^{\frac{1}{2}} I^{\frac{1}{4}}(\mu J_o \rho)^{\frac{1}{4}}. \tag{5}$$

Here, z is the distance from the cathode, h is the enthalpy of the arc core, μ is the permeability, J_o is the current density at the cathode, ρ is the density, and E is the electric field. Solving equation (1-5) iteratively together with the material data of nitrogen enable calculation of the arc temperature, radius, and the electric field. In some cases, due to scarcity of high pressure material data for nitrogen at high temperature, thermodynamic and transport properties of high pressure air are used [19-21]. From the calculated electric field, the arc voltage can then be estimated by assuming a fixed electrode voltage drop of 17 V for all filling pressures, based on previous works [9], [22].

The calculated arc temperature and radius for free-burning arcs at different filling pressures are plotted in Fig. 5(a). It can be seen that the free-burning arc radius decreases from approximately 4 mm for atmospheric pressure arcs to approximately 1.5 mm and 1.35 mm for arcs burning at 20 bar and 80 bar filling pressures, respectively. The calculated arc temperature for free-burning arcs at different pressure levels lies in the range of 9,000-12,000 K. The temperature in the arc increases when the pressure rises from 1 bar to 20 bar mainly due to constriction. The slight decrease in temperature for 40 bar and 80 bar is due to the increased radiative cooling of the arc [17]. The calculated arc voltages for free-burning arcs, at different filling pressures are in good agreement with the measured values and are plotted in Fig. 5(b).

B. Tube-constricted Arc

Ablation controlled arcs at atmospheric pressure have been studied in the past [11-13]. The contraction factor which is the ratio of the cross sectional area of the arc and the tube is calculated based on the analytical expression described in the works of Kovitya [23]:

$$\frac{A}{Q} = \frac{(1-f)\rho_c a_c}{\left(\frac{f}{h_c} - \frac{1-f}{h-h_c}\right)\rho(h-h_c)a + (1-f)\rho_c a_c}. \tag{6}$$

Here, A is the arc cross sectional area, Q is the cross sectional area of the tube, h is the enthalpy of the arc, a is the speed of sound, ρ is the mass density, and f is the parameter determining the part of radiation causing ablation. The subscript c denotes the properties in the vapor region, while without subscript denotes the arc core. The value of f lies in the range of 0 to 1 and can ideally be determined from the measured mass loss of the tube due to ablation. The mass losses in these cases are believed to be extremely small and were not measured. In this paper, f is chosen in such a way that the calculated arc voltage matches the measured arc voltage. The steady state solution of the two zone model is determined for an arc current of 150 A. Conservation of mass, momentum, and energy along with Ohm's law is used to calculate the arc temperature and radius of the tube-constricted arc [23]. As the arc voltage dependency on tube material was not found to be strong at high filling pressures, only the alumina was considered for the tube-constricted arcs. The two-zone arc model is not valid when the tube diameter is very large compared to the free-burning arc diameter. Hence, only 2 mm, 4 mm, and 8 mm tube inner diameters are considered here. The equations along with the material dependent data of electrical conductivity, density, enthalpy, sonic velocity are solved iteratively [19], [21], [24].

Due to the constriction of the tube, the arc radius decreases and the temperature in the core increases. Fig. 6 shows the calculated arc temperature and radius for the arcs burning inside alumina tube as a function of filling pressure. The free-burning arc radius at atmospheric pressure was previously calculated to be approximately 4 mm with an arc core temperature of approximately 9,000 K. At atmospheric pressure, the tube constricts the arc and subsequently the arc temperature increases up to approximately 19,000 K. An increase in arc temperature generally results in a higher electrical conductivity.

This is the accepted version of an article published in IEEE Transactions on Plasma Science
DOI: 10.1109/TPS.2018.2880841

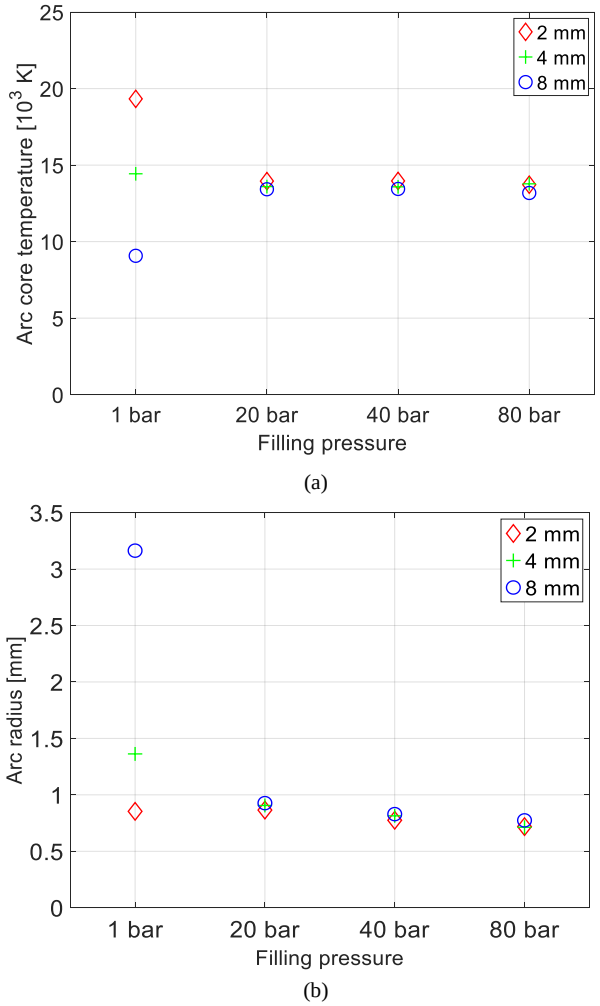

Fig. 6. Calculated arc temperature and radius for arc current of 150 A burning inside different diameter of alumina tube as a function of filling pressures. (a) Arc temperature. (b) Arc radius.

However, due to the tube-constriction at atmospheric pressure, the arc area is reduced. Hence, the arc voltage increases as the tube diameter decreases when the arc burns in atmospheric pressure.

At higher filling pressures (i.e., 20 bar, 40 bar, and 80 bar), the effect of the tube inner diameter on the arc radius and temperature is not as strong as at atmospheric pressure. The filling pressure alone constricts the arc when the pressure is increased, as was seen for the free-burning arcs (see Fig. 5(a)). As a result, the effect of the tube constriction is less significant at higher filling pressures. The arc temperature remains almost constant around 14,000 K for filling pressures above 20 bar irrespective of the tube diameters. The arc radius decreases slightly with filling pressure, while the effect of tube diameter is not strong when the gas pressure is above 20 bar.

From the experimental results, as the filling pressure was increased, the relationship between the arc voltage and tube diameter was not as straightforward as for the atmospheric pressure arcs. As the arc is constricted due to the filling pressure, the radiation emission coefficient increases [25]. For not optically thin plasmas with a radius of 1 mm at 15,000 K, the net emission coefficient becomes approximately 10 times larger when the pressure is increased from 1 bar to 100 bar [25]. However, the increase in filling pressure also accounts for a larger number of molecules outside the arc core, resulting in higher absorption rates of the radiated energy. As a result, the absorption coefficient increases with the filling pressure. The absorption coefficient becomes approximately 100 times larger when the filling pressure is increased from 1 bar to 100 bar at an arc temperature of 15,000 K [25]. This clearly demonstrates the dominant effect of absorption over radiation at high filling pressures. A similar dominance of absorption coefficient over net radiation emission coefficient at elevated pressures has also been reported for hydrogen arcs burning at 20 bar gas pressure [26]. Likewise, a significant reduction of ablation in metal by a laser due to increased pressure of the surrounding gases has been reported in the literature [27]. This agrees with the optical micrographs, where less scar marks were observed at the inner surfaces of the tubes at 80 bar, compared to atmospheric pressure.

For arcs burning in a 2 mm diameter tube, the measured arc voltages were lower than those in 8 mm tube diameters at 40 bar and 80 bar filling pressures. The viscosity could play a vital role in these cases. The fluid flow resistance inside a tube is linearly proportional to viscosity and inversely proportional to the power of four of the tube radius in case of a laminar flow. The type of flow occurred inside the tube is beyond the scope of this study. Nevertheless, the viscosity of air plasma increases approximately 15 times at the calculated arc temperatures when the filling pressure of the air is increased from 1 bar to 80 bar [20]. Consequently, for tubes with inner diameter of 2 mm at 40 and 80 bar filling pressures, a highly conductive plasma may fill the tube due to high flow resistance, which can play a pivotal role to increase the conductivity of the arc channel.

To summarize, the arc radii and temperatures were calculated using Lowke's theory of free-burning arcs. The arc is constricted by increasing gas pressure. The arc radius and the temperature for the arcs burning inside alumina tubes with 2, 4, and 8 mm inner diameters were then calculated for different filling pressures based on the two-zone arc model. The effect of tube constriction is apparent at 1 bar ambient pressure. However, the effect of tube inner diameter (2, 4, 8 mm) on the arc temperature and radius are found less significant at high filling pressures (i.e., 20 bar, 40 bar, and 80 bar). The increased absorption of arc energy by the gas surrounding the arc core reduces the radiation reaching the inner surface of the tube at high filling pressures, which is also consistent with the observation from optical micrographs. Finally, for the tubes with 2 mm inner diameter at gas pressures of 40, and 80 bar, the effect of viscosity could play a crucial role in the reduced arc voltage.

V. Conclusion

Nitrogen arcs burning inside cylindrical tubes of alumina and PTFE have been investigated experimentally by means of arc voltage measurements at different filling pressures, including supercritical region. Moreover, optical microscopy has been used to qualitatively investigate the level of ablation. Based on

This is the accepted version of an article published in IEEE Transactions on Plasma Science
DOI: 10.1109/TPS.2018.2880841

the experimental results and calculated arc parameters, the following conclusions have been drawn:

- At atmospheric pressure, the arc voltage increases with decreasing inner diameter of the tube, as expected.
- The measured arc voltage at high filling pressures inside a tube does not have a simple relationship with the inner diameter of the tube. The filling pressure constricts the arc channel, which limits the interaction of the arc core with the tube.
- The optical micrographs show reduced ablation traces in a 4 mm wide tube at 80 bar compared to the 1 bar ambient pressure arcs. The increase in the absorption of radiation by the gas surrounding the arc core at very high pressure reduces the ablation. As a result, ablation may become less significant for ultrahigh-pressure nitrogen arcs in contrast to the atmospheric pressure arcs.

REFERENCES

[1] T. Hazel, H. H. Baerd, J. J. Legeay, and J. J. Bremnes, "Taking power distribution under the sea: design, manufacture, and assembly of a subsea electrical distribution system," *IEEE Industry Applications Magazine*, vol. 19, no. 5, pp. 58-67, 2013.

[2] J. Sengers and J. L. Sengers, "Thermodynamic behavior of fluids near the critical point," *Annual Review of Physical Chemistry*, vol. 37, no. 1, pp. 189-222, 1986.

[3] J. Zhang, A. Markosyan, M. Seeger, E. van Veldhuizen, E. van Heesch, and U. Ebert, "Numerical and experimental investigation of dielectric recovery in supercritical N_2," *Plasma Sources Science and Technology*, vol. 24, no. 2, p. 025008, 2015.

[4] T. Ito and K. Terashima, "Generation of micrometer-scale discharge in a supercritical fluid environment," *Applied physics letters*, vol. 80, no. 16, pp. 2854-2856, 2002.

[5] E. H. Lock, A. V. Saveliev, and L. A. Kennedy, "Influence of electrode characteristics on DC point-to-plane breakdown in high-pressure gaseous and supercritical carbon dioxide," *IEEE Transactions on Plasma Science*, vol. 37, no. 6, pp. 1078-1083, 2009.

[6] H. Tanoue *et al.*, "Characteristics of shock waves generated by a negative pulsed discharge in supercritical carbon dioxide," *IEEE Transactions on Plasma Science*, vol. 42, no. 10, pp. 3258-3263, 2014.

[7] Z. Yang, S. Hosseini, T. Kiyan, S. Gnapowski, and H. Akiyama, "Post-breakdown dielectric recovery characteristics of high-pressure liquid CO_2 including supercritical phase," *IEEE Transactions on Dielectrics and Electrical Insulation*, vol. 21, no. 3, pp. 1089-1094, 2014.

[8] J. Zhang, B. van Heesch, F. Beckers, T. Huiskamp, and G. Pemen, "Breakdown voltage and recovery rate estimation of a supercritical nitrogen plasma switch," *IEEE Transactions on Plasma Science*, vol. 42, no. 2, pp. 376-383, 2014.

[9] F. Abid, K. Niayesh, E. Jonsson, N. S. Støa-Aanensen, and M. Runde, "Arc Voltage Characteristics in Ultrahigh-Pressure Nitrogen Including Supercritical Region," *IEEE Transactions on Plasma Science*, vol. 46, no. 1, pp. 187-193, 2018.

[10] P. Kovitya, "Ablation-stabilized arcs in nylon and boric acid tubes," *IEEE transactions on plasma science*, vol. 15, no. 3, pp. 294-301, 1987.

[11] P. Kovitya and J. Lowke, "Theoretical predictions of ablation-stabilised arcs confined in cylindrical tubes," *Journal of Physics D: Applied Physics*, vol. 17, no. 6, pp. 1197-1212, 1984.

[12] L. Muller, "Modelling of an ablation controlled arc," *Journal of Physics D: Applied Physics*, vol. 26, no. 8, p. 1253, 1993.

[13] C. Ruchti and L. Niemeyer, "Ablation controlled arcs," *IEEE Transactions on Plasma Science*, vol. 14, no. 4, pp. 423-434, 1986.

[14] M. Seeger, J. Tepper, T. Christen, and J. Abrahamson, "Experimental study on PTFE ablation in high voltage circuit-breakers," *Journal of Physics D: Applied Physics*, vol. 39, no. 23, pp. 5016-5024, 2006.

[15] F. Abid, K. Niayesh, E. Jonsson, N. S. Støa-Aanensen, and M. Runde, "Arc Voltage Measurements Of Ultrahigh Pressure Nitrogen Arcs In Cylindrical Tubes," presented at the 22nd International Conference on Gas Discharges and their Applications, Novi Sad, Serbia, 2-7 September, 2018.

[16] J. Aakervik, G. Berg, and S. Hvidsten, "Design of a high voltage penetrator for high pressure and temperature laboratory testing," in *Electrical Insulation and Dielectric Phenomena (CEIDP)*, Cancun, Mexico, 16-19 Oct. 2011, pp. 267-270: IEEE.

[17] J. Lowke, "Simple theory of free-burning arcs," *Journal of physics D: Applied physics*, vol. 12, no. 11, p. 1873, 1979.

[18] L. Niemeyer, "Evaporation dominated high current arcs in narrow channels," *IEEE Transactions on power Apparatus and Systems*, vol. PAS-97, no. 3, pp. 950-958, 1978.

[19] W. Chunlin *et al.*, "Thermodynamic and transport properties of real air plasma in wide range of temperature and pressure," *Plasma Science and Technology*, vol. 18, no. 7, p. 732, 2016.

[20] A. D'Angola, G. Colonna, A. Bonomo, D. Bruno, A. Laricchiuta, and M. Capitelli, "A phenomenological approach for the transport properties of air plasmas," *The European Physical Journal D*, vol. 66, no. 8, p. 205, 2012.

[21] K. Meher, N. Tiwari, and S. Ghorui, "Thermodynamic and transport properties of nitrogen plasma under thermal equilibrium and non-equilibrium conditions," *Plasma Chemistry and Plasma Processing*, vol. 35, no. 4, pp. 605-637, 2015.

[22] Y. Yokomizu, T. Matsumura, R. Henmi, and Y. Kito, "Total voltage drops in electrode fall regions of, argon and air arcs in current range from 10 to 20 000 A," *Journal of Physics D: Applied Physics*, vol. 29, no. 5, p. 1260, 1996.

[23] P. Kovitya and J. Lowke, "Theoretical predictions of ablation-stabilised arcs confined in cylindrical tubes," *Journal of Physics D: Applied Physics*, vol. 17, no. 6, p. 1197, 1984.

[24] P. Kovitya, "Thermodynamic and transport properties of ablated vapors of PTFE, alumina, Perspex, and PVC in the temperature range 5000-30 000 K," *IEEE Transactions on plasma science*, vol. 12, no. 1, pp. 38-42, 1984.

[25] J. Zhong, F. Yang, W. Wang, D. Yuan, and J. D. Yan, "Net Emission Coefficient and Radiation Transfer Characteristics of Thermal Plasma Generated in Nitrogen-PTFE Vapor Mixture," *IEEE Transactions on Plasma Science*, vol. 46, no. 4, pp. 990-1002, 2018.

[26] P. Gueye, Y. Cressault, V. Rohani, and L. Fulcheri, "A simplified model for the determination of current-voltage characteristics of a high pressure hydrogen plasma arc," *Journal of Applied Physics*, vol. 121, no. 7, p. 073302, 2017.

[27] Y. Chivel and V. Nasonov, "Influence of ambient gas pressure on laser induced metal ablation," *Physics Procedia*, vol. 5, pp. 255-259, 2010.

Fahim Abid received the B.Sc. degree in electrical and electronic engineering from the Islamic University of Technology (IUT), Dhaka, Bangladesh in 2012. He received the M.Sc. degree in electrical engineering combinedly from Royal Institute of Technology (KTH), Stockholm, Sweden and Technical University Eindhoven (TU/e), Eindhoven, Netherlands in 2015. He is currently working as a PhD candidate at the department of electric power engineering in Norwegian University of Science and Technology (NTNU), Trondheim, Norway.

This is the accepted version of an article published in IEEE Transactions on Plasma Science
DOI: 10.1109/TPS.2018.2880841

Kaveh Niayesh (S'98–M'01–SM'08) received the B.Sc. and M.Sc. degrees in electrical engineering from the University of Tehran, Tehran, Iran, in 1993 and 1996, respectively, and the Ph.D. degree in electrical engineering from the RWTH-Aachen University of Technology, Aachen, Germany, in 2001.

He held different academic and industrial positions including Principal Scientist with the ABB Corporate Research Center, Baden-Dattwil, Switzerland; Associate Professor with the University of Tehran; and Manager, Basic Research, with AREVA T&D, Regensburg, Germany. Currently, he is a Professor with the Department of Electric Power Engineering, Norwegian University of Science and Technology (NTNU). He is the holder of 16 patents and has more than 105 journal and conference publications on current interruption and limitation, vacuum and gaseous discharges, plasma modeling and diagnostics, switching transients, and pulsed power technology.

Nina Sasaki Støa-Aanensen received the M.Sc. degree in applied physics and mathematics and the Ph.D. degree in electrical power engineering from the Norwegian University of Science and Technology (NTNU), Trondheim, Norway, in 2011 and 2015, respectively.

She is currently working with SINTEF Energy Research, Trondheim, Norway.